Some recent studies with the solid-ionomer electrochemical capacitor

S. Sarangapani*, **J. Forchione**, **A. Griffith** and **A. B. LaConti**
Giner, Inc., 14 Spring Street, Waltham, MA 02254-9147 (U.S.A.)

R. Baldwin
NASA Lewis Research Center, Cleveland, OH 44135 (U.S.A.)

Abstract

Giner, Inc. has developed a high-energy-density, all-solid-ionomer electrochemical capacitor, completely free of liquid electrolyte. The novel features of this device include (i) a three-dimensional metal oxide-particulate-ionomer composite electrode structure and (ii) a unitized repeating cell element. The composite electrode structures are bonded to opposite sides of a thin sheet of a solid proton-conducting ionomer membrane and form an integrally bonded membrane and electrode assembly (MEA). Individual MEAs can be stacked in series as bipolar elements to form a multiple cell device. The discharge characteristics and energy storage properties of these devices are described. Typical capacitance measured for a unit cell is 1 F/cm^2. Life testing of a multicell capacitor on an intermittent basis has shown, that over a 10 000 h period, the capacitance and resistance of the cell has remained invariant. There has been no maintenance required on the device since it was fabricated. Other multicell units of shorter life duration have exhibited similar reliable performance characteristics. Recent work has focused on increasing the capacitance of the unitized structure and improving the low-temperature characteristics. The approaches and experimental results will be presented. Some possible advanced NASA applications for these unique all-solid-ionomer devices will be discussed.

Introduction

Electrical pulse power generating systems include electrostatic (dielectric) and electrochemical capacitors. The former accumulate substantial energy only by developing a very high voltage difference across the dielectric gap. These very high potentials make them impractical for certain battery/capacitor high-energy-density pulse power applications. Electrochemical capacitors, on the other hand, can accumulate substantial charge (and deliver it within the required times) at much lower voltages, compatible with the voltage of batteries. The classical 'electrochemical supercapacitor' is a symmetric device in which the electrolyte is placed between two identical electrode systems (i.e. with the same electrode material under similar conditions causing the same process in each electrode but occurring in opposite direction). Pragmatically, the term 'electrochemical capacitors' can be extended to asymmetric

*Author to whom correspondence should be addressed.

0378-7753/91/$3.50

devices, i.e. devices with different electrode reactions at each electrode, although these latter devices may be closer to an ultra-high-power battery.

Symmetric electrochemical capacitors show respectable capacities from the double layer charging of their electrodes, which act as 'perfectly polarizable electrodes' (i.e. electrodes which can operate in an extended potential range without a faradaic reaction). Considerably higher capacities are obtained, however, with electrode systems having a substantial potential region over which a faradaic reaction takes place at a potential which depends more or less linearly, and reversibly (independent of the value of the current and without substantial hysteresis) on the charge that is transferred between the phases. The charge versus potential slope represents the 'pseudo capacity' of the system, which can be considerably higher than the capacity of the double layer (i.e. of a purely capacitative electrode interface). Since an electrochemical capacitor cell is made of two capacitors in series, each representing one electrode–electrolyte interface, the overall capacity of the cell is one-half the capacity of the individual electrode interface. But the stored energy is augmented by the cell voltage being twice that of the single electrode interface.

Symmetric electrochemical capacitors have electrical behavior similar to electrostatic capacitors. Of particular relevance to the proposed work is the question of energy (E) delivered by the capacitor, which is related to the integral capacity (C) and initial potential (V_i) and the final potential (V_f) of the capacitor by the expression:

$$E = \frac{1}{2} C[V_i^2 - V_f^2] \tag{1}$$

or

$$E = \frac{1}{2} CV_i^2[1 - \alpha^2] \tag{2}$$

where α is the fraction of the initial voltage retained in the capacitor. If the internal resistance of the capacitor (R_i) is not negligible when compared with the external resistance (R_e), and both of these resistances are constant, the useful energy (E_u) is given by:

$$E_u = \frac{1}{2} CV_i^2[1 - \alpha^2] \frac{R_e}{R_e + R_i} \tag{3}$$

For the purpose of the following comparison of the energy of symmetric and asymmetric devices, the supercapacitor's energy can be expressed as a function of the charge, Q, which can be obtained by the complete discharge of the capacitor ($Q = CV_i$). Accordingly, eqn. (2), for instance, can be converted to:

$$E = \frac{1}{2} QV_I[1 - \alpha^2] \tag{4}$$

Symmetric electrochemical capacitors have a number of characteristics not exhibited by dielectric capacitors. As mentioned above, electrochemical capacitance is orders-of-magnitude higher than dielectric capacitance. On the other hand, they have a relatively low limit to the voltage that they can tolerate before undesired reactions (e.g. H_2O electrolysis) occur.

Asymmetric devices have different reactions at each cell electrode. The reactions can be (i) both capacitative in nature, (ii) one capacitative and the other battery-like or (iii) both battery-like. The latter type represents an ultra-high power battery. The high-power characteristic can be obtained by the selection of materials with very reversible reactions (such as proton insertion in NiO to produce NiOOH, or in Raney nickel, or in palladium to give a hydride) and by spreading the active materials over large electrode areas so that ohmic resistances within the electrodes, and the mass diffusion within the active material, are low.

The main advantage of the ultra-high-power battery is that it delivers the energy at a substantially invariant potential. Its energy is related to charge and voltage by

$$E = QV_i \tag{5}$$

Comparison of eqns. (4) and (5) shows that the energy obtained from the ultra-high-power battery operating at a voltage, V, is $2/(1-\alpha^2)$ larger than that of the ultra-capacitor with the same initial voltage, V.

In principle, the potential electrochemical limitations of the supercapacitor discussed above apply to the ultra-high-power battery. In practice a specific system has to be selected with very high reversibility (e.g. a system involving only simple proton insertion reactions), with very low internal resistance, etc.

Review of prior work

Carbon capacitors

One of the first electrochemical capacitors developed had carbon paste electrodes and liquid sulfuric acid electrolyte, together with a microporous separator. Relatively thick (36 mil) electrodes were used to get 2 F/cm^2 capacitance from this system at low frequencies and/or low charge/discharge rates [1]. Later developments in electrode technology for the acid electrolyte electrochemical capacitor included lead counter electrodes [2] and polyoxometallate-deposited carbon paste electrodes, stabilized with an organic amine [3]. These modifications add either additional weight or manufacturing complexity to the capacitor system and resulted in poor stability during cycling.

Several workers have attempted to improve the performance of carbon-based electrochemical capacitors [4–7]. Currie investigated several carbons with different micropore volumes and compared the performance of H_2SO_4 and K_2SO_4 as electrolytes. An improvement in capacity with micropore surface area was noticed and the self-discharge rate was significantly reduced with

K_2SO_4 electrolyte. A drawback of the later approach was the considerable increase in internal series resistance with the neutral electrolyte.

Researchers at Space Power Institute, Auburn University have been conducting research to minimize series resistance in carbon-based capacitor systems [5, 6]. They point out that one of the main drawbacks of carbon black as electrode material is its high resistivity arising out of poor particle-to-particle contact. The energy density (kJ/kg) is directly proportional to accessible surface area of electrode materials, and carbon black is the only known electrode material with surface areas in the range 1000–2000 m^2/g. They show that the series resistance can be decreased considerably by making a composite of nickel or stainless steel fiber (20 μm in diameter) and carbon black/fibers. More than an order-of-magnitude improvement in capacitance for unit weight is realized by this approach.

Noble metal capacitors

Oxides of noble metals, mostly RuO_2, have been investigated extensively as an electrode material. RuO_2 has a high capacity of about 150 μF/real cm^2 [8]. This is substantial due to pseudocapacity from surface reaction, which can be written approximately as:

$$2RuO_2 + 2H^+ + 2e^- \longrightarrow Ru_2O_3 + H_2O \quad (6)$$

This type of surface reaction, in combination with double-layer processes, has been shown to be capable of sustaining high current densities on the millisecond scale [9, 10]. RuO_2 can be made into a high-surface-area coating [11] or as high-surface-area particulates [12]. Bonding of particulates to an ionomer membrane has been demonstrated for RuO_2 anodes for use in chlor-alkali cells [13] where membrane and electrode assemblies with active areas of up to 35 ft^2 have been prepared.

Craig [14] describes a supercapacitor based on ruthenium oxide and mixtures of Ru and Ta oxides, and reported capacitances as high as 2.8 F/cm^2.

Sierra Alc-zar *et al.* [15] have described an electrochemical capacitor cell using high-surface-area RuO_2 having a surface roughness (real area/geometric area) of greater than 10 000; this device used a liquid sulfuric acid electrolyte.

Other researchers have worked to increase the capacitance of electrode structures. A summary of some of the most applicable work is as follows.

The works of Craig, Pinnacle Research, and Giner, Inc. with RuO_2-based systems are attempts to improve the power output of capacitors while improving the charge storage capacity by one or two orders of magnitude. McHardy *et al.* [16, 17] at Hughes reported essentially on a similar system with IrO_2 as the electrode material, except that they paired it with a Pt/H system. This is fundamentally different from an electrochemical capacitor. The Pt–H electrode uses the fast electrode kinetics of the hydrogen reaction and the large pseudocapacitance associated with adsorbed hydrogen. The IrO_2 electrode is essentially the same as RuO_2 except that it has higher

charge density and power capability, if properly prepared. McHardy *et al.* report a typical capacity of 20 mC/cm^2 for their Pt–H/IrO_2 system for 5 ms pulses.

Rauh [18] investigated IrO_2, and to a lesser degree RuO_2, as part of a program to screen several materials for pulse power applications. A sputtered IrO_2 film gave 11 mF/cm^2 for 0.1 μm thickness; a 5-μm film of thermally prepared IrO_2 gave 35 mF/cm^2.

Non-noble metal oxide capacitors

Rauh [19] investigated a nickel oxide film in combination with $LaNi_5$ as the hydrogen electrode. Sputtered, electrochemical and chemical nickel oxides were examined — only electrochemically formed oxide gave significant capacity. Several problems of scaling up these systems were noted which included current distribution, resistive/inductive losses, heat rejection, side reactions and limited cycle life for pulse power applications.

A recent investigation of the nickel oxide electrode was by the GM research labs [20]. A nickel–zinc battery designed for electric vehicles was tested for pulse power capabilities in this work. The power output was limited by the nickel oxide electrode, and depended on the state of charge of the battery. While sintered nickel oxide electrodes showed no degradation after 300–500 deep discharge cycles, pocket-type nickel oxide electrodes showed severe power capability degradation after only several cycles.

Rauh [18] also investigated WO_3. This and other hydrous oxide films they claim, take advantage of both non-faradaic and faradaic processes. For example, a 1 μm thick WO_3 film should give 22 mF/cm^2 in non-faradaic capacitance and 220 mF/cm^2 in faradaic capacitance. This translates into an energy density of 7.8 W h/lb (258 kJ/l) and a power density of 434 kW/lb (1500 kW/l). Thicker films, unfortunately, do not appear to have linear scaling of capacity.

Craig, in his patent application [14], has also claimed supercapacitance behavior (in cyclic voltammetry studies) with metal oxides such as Mo, W, Co and Ni.

Several other battery systems such as Li/metal sulfide, Li/SO_2, Pb/acid and several conducting polymer based systems have been investigated as pulse power sources. These suffer from either inadequate safety, poor cycle life or low power capabilities.

Non-aqueous capacitors

Non-aqueous solutions, such as propylene carbonate with a dissolved salt have been used in capacitors. These electrolytes have been successfully used in the low-rate Dynacap capacitor [7] to achieve single-cell voltage of up to 2.8 V with a specific capacitance of 100 F/g. They are limited for pulse power applications because of their low conductivity. Also there is concern about the long-term stability of these materials.

Capacitors based on conducting polymers

Conducting polymers are a class of materials that have interesting possibilities for capacitor applications. Polyaniline polymer films formed on Pt and nickel foils have been used as supercapacitor devices. Stability problems of these polymers appear to limit the cycle life at the present stage of development. In addition, they typically exhibit a much higher resistance.

Polyaniline is an electronic conductor only when immersed in acid electrolyte, between 0.2 and 0.8 V (versus SCE) [21]. Gottesfeld *et al.* [22] reported a capacitance of 800 Coulombs/cm^3 in aqueous acidic electrolyte for a 10–60 nm polyaniline film, cycling between 0 and 0.55 V (versus Ag wire). In recent work, Bhakta *et al.* [23] described conductive polymers for use in super capacitors based on aniline copolymers. Polymer films were formed on Nafion coated platinum and nickel substrates using different aniline derivatives.

Device concept and device fabrication

The device concept and fabrication methods are fully explained in earlier publications [24, 25]. The capacitor includes (i) a three-dimensional metal oxide-particulate-ionomer composite electrode structure, whereby the ionomer coats the individual particles and provides a mechanism for continuous proton transport throughout the composite structure and (ii) a unitized repeating cell element that includes this three-dimensional composite electrode structure.

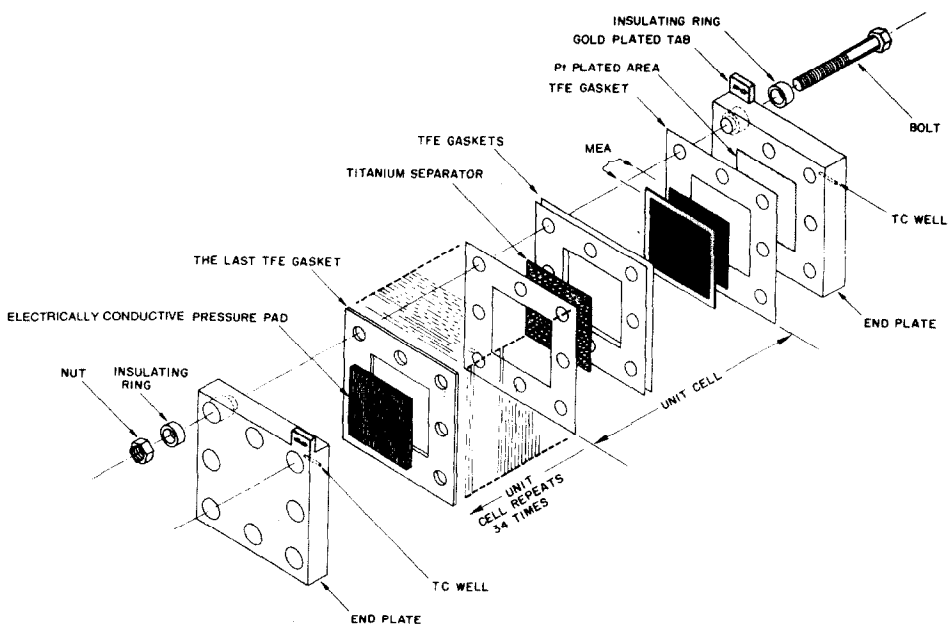

Fig. 1. Exploded schematic view of capacitor cell components.

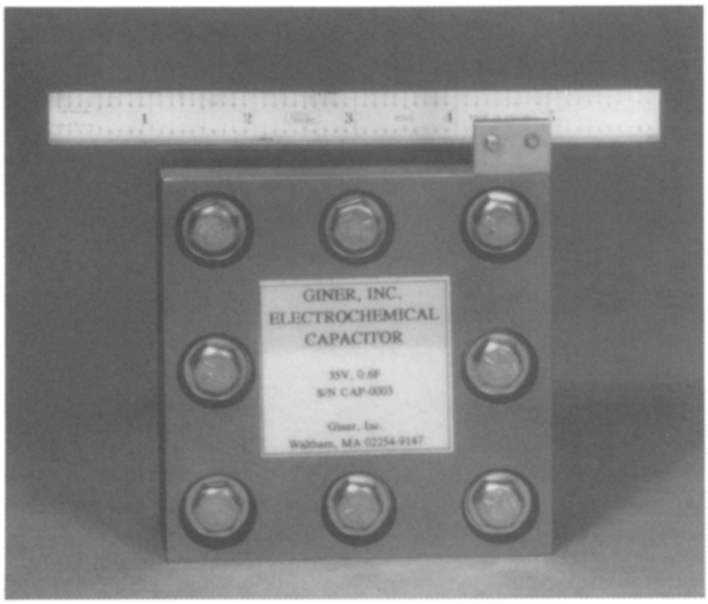

Fig. 2. Giner, Inc. 35-cell PEM electrochemical capacitor.

The composite electrode structures are bonded to opposite sides of a thin sheet of a solid proton-conducting ionomer membrane such as the Dow XUS 13204.10 and form an integrally bonded membrane and electrode assembly (MEA). An exploded view of the cell components and assembly of a 35-cell stack are shown in Fig. 1. In this device, the membrane electrode assemblies (MEAs) are stacked in a bipolar arrangement. An electrically conductive pressure pad is used at one end to ensure isostatic conditions on all MEAs. The assembly is held in place using titanium bolts and nuts, torqued to the desired force. A photograph of this device is shown in Fig. 2.

Experimental and discussion

Capacitance test consisted of discharging the MEA across a 10 Ω load and measuring the RC time constant – the time to decay from 0.9–0.331 V (0.9/e). The MEA was charged to a potential of +1.000 V using a PAR 173 potentiostat/galvanostat in conjunction with a PAR 276 interface. The cell was then disconnected and allowed to discharge across a 10 Ω load while the PAR 276 recorded the voltage decay curve. Internal resistance was determined by applying a square wave current pulse of ±0.5 A, 100 Hz and measuring the instantaneous voltage decay at the break points. The data presented in Tables 1–4 were obtained by charging the 5-cell unit at constant current to 5 V, holding the cell at 5 V or *OCV* for a specified time and subsequently discharging into a selected load resistor.

TABLE 1

Effects of discharge resistor on the energy efficiency of PEM electrochemical capacitor 5-cell unit

I_{chg} (mA)	R_L (Ω)	Charge time at constant I (s)	Hold time at constant V (s)	Energy in constant I (J)	Energy out (J)	Efficiency (%)	Discharge time to V(0)/e (s)
500	10	39.7	0	55.8	46.1	83	41.1
500	1.0	40.1	0	56.8	37.9	67	4.0
500	0.14 ± 0.01	39.5	1	55.4	17.8	32	0.20

TABLE 2

Effects of constant current charge rate on the energy efficiency of PEM electrochemical capacitor 5-cell unit

R_L (Ω)	I_{chg} (mA)	t_{chg} (s)	t_{hold} (s)	$(E_{in})_I$ (J)	$(E_{in})_V$ (J)	E_{out} (J)	Efficiency (%)	Discharge time to V(0)/e (s)
1.0	300	69.1	1.1	59.4	0.8	38.3	64	4.0
1.0	500	39.3	6.0	55.3	5.0	37.9	63	4.2
1.0	1000	21.3	1.1	54.2	2.0	36.0	64	4.1
1.0	1000	18.7	1.4	52.8	3.4	37.3	66	3.9

TABLE 3

Effects of open-circuit hold time on the energy efficiency of PEM electrochemical capacitor 5-cell unit

$(t_{chg})_I$ (s)	$(t_{hold})_{OCV}$ (s)	$(E_{in})_I$ (J)	E_{out} (J)	Efficiency (%)	Discharge time to V(0)/e (s)
38.6	0	53.7	38.9	72	3.9
37.8	10.9	53.3	36.1	68	4.1
38.4	20.5	53.5	34.2	64	4.2
38.2	60.5	53.7	32.2	60	4.2
38.8	199.0	54.1	31.2	58	4.8
38.9	301.9	54.5	29.7	54	4.9

Performance and life test results of multicell stacks

Breadboard capacitor stacks containing 5, 10 and 35 cells were fabricated, as shown in Fig. 1, using Nafion-coated RuO_x particulate electrodes bonded to Dow XUS 13204.10 membranes. Individual (unit) cell area was 25 cm^2. Typical capacitance per unit cell ranged from 0.7–1 F/cm^2. The results of cycle testing (up to 1500 cycles) of the 5-cell unit on a 60 s charge/discharge

TABLE 4

Effects of temperature on the energy efficiency of PEM electrochemical capacitor 5-cell unit

Temperature (°C)	t_{chg} (s)	t_{hold} (s)	$(E_{in})_I$ (J)	E_{out} (J)	Efficiency (%)	Discharge time to V(0)/e (s)
−4	27.2	2.8	42.3	12.3	29	1.1
10	40.1	0	56.3	34.1	61	4.1
25	40.1	0	56.8	37.9	67	4.0
46	47.2	0	64.1	42.3	66	4.4

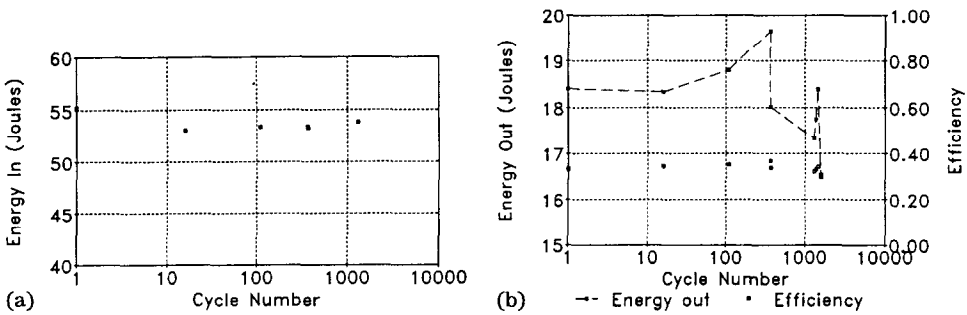

Fig. 3. Cycle testing of 5-cell unit on a 60 s charge/discharge cycle. (a) Energy expended during charging as a function of cycles. (b) Output energy efficiency during discharge as a function of cycles.

cycle are shown in Fig. 3 together with the energy efficiency. The unit was charged at a constant current of 0.6 A to 5 V, then, after about an 8 s live hold, the unit was discharged into a 0.134 Ω load. This was repeated at 60 s intervals until 1574 cycles were completed. For nine of the cycles energy input and output were recorded. The energy efficiency for this very high load is ∽35%. While part of the efficiency loss is due to *IR* dissipation, a significant portion of the energy loss can be attributed to slow discharge processes, which may be the charge/discharge of the inner core of the RuO_x particles. The efficiency improves to 82% for a 10 Ω load and about 89% for a 100 Ω load (Table 1). Charging rate does not seem to affect the energy efficiency appreciably at moderate rates (Table 2). The self-discharge behavior (or leakage current) is illustrated in Table 3. Comparison of these data with that presented in Table 1 shows that approximately 15% of the energy is lost for a holding time of 5 min. The effect of temperature on capacitor efficiency is shown in Table 4. Efficiency decreases from approximately 66 to 61% as the temperature decreases from 46 to 10 °C. At −4 °C, the efficiency decreases dramatically to 29%. The approach to decreasing this efficiency loss at low temperatures is discussed in a subsequent section.

Figure 4 shows the capacitance and resistance of the 5- and 35-cell units as a function of time. Both the capacitance and resistance are steady over the duration of the test which is over a year for the 5-cell unit.

Figure 5 shows the gravimetric and volumetric power densities of our capacitors as a function of pulse width. For a 0.7 V cutoff, power densities as high as 2×10^3 W/kg and 4×10^4 W/l can be obtained for 5 ms pulses. This result can be improved further as the specific capacitance of these devices are increased as discussed below.

Approaches to increasing energy density

The maximum capacitance that has been realized currently with the RuO_x* 100 m^2/g Nafion-coated structures [24, 25] is in the range of 75–80

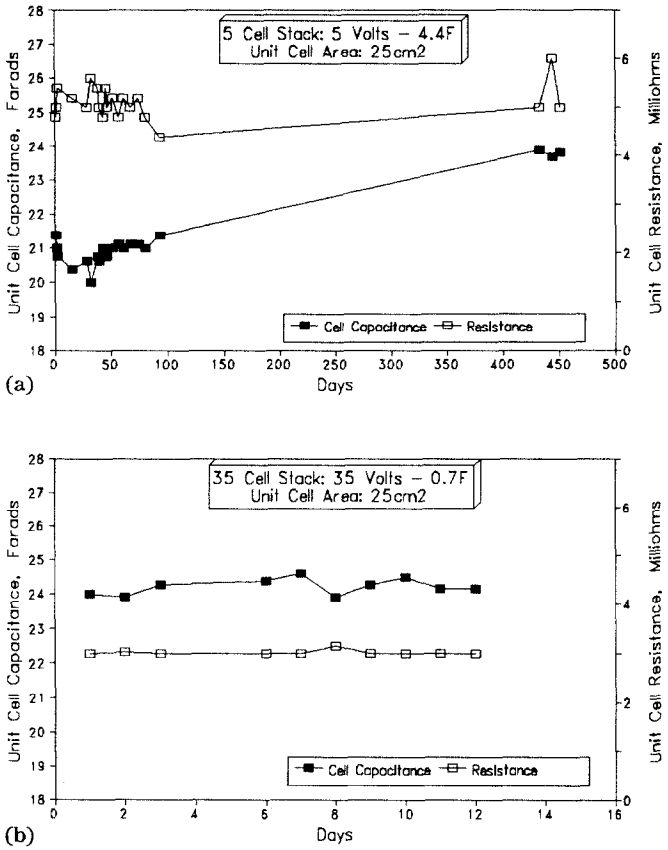

Fig. 4. Cell capacitance and resistance as a function of days of cell operation: (a) 5-cell stack; (b) 35-cell stack.

*Technically, RuO_x is a more correct expression of the chemical compound than RuO_2 since the x value can range from 1.9 to above 2.0. In addition, the charging/discharging cycle of the capacitor may cause variations in the oxidation state of the compound.

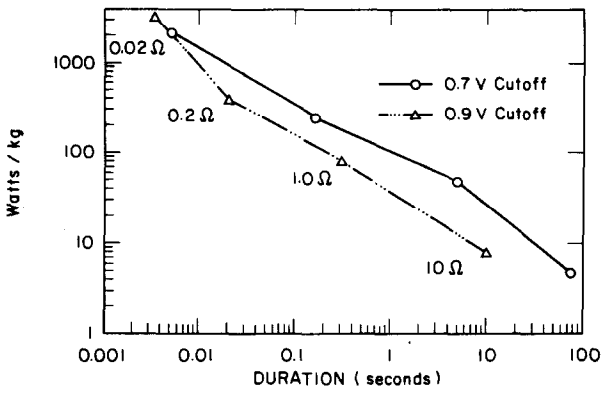

(a)

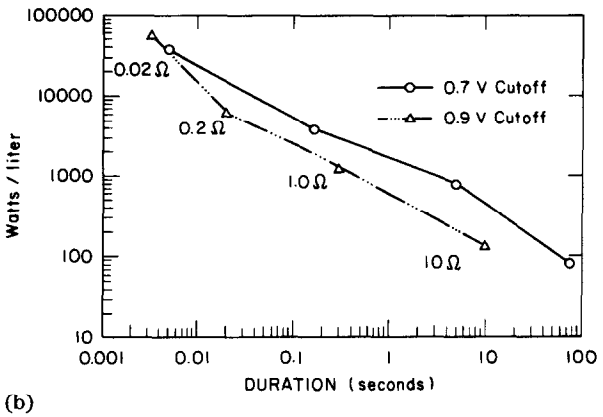

(b)

Fig. 5. Power density as a function of pulse duration for Giner, Inc. PEM capacitor: (a) gravimetric power density; (b) volumetric power density.

F/g. Calculations based on 150 μF/cm^2 show that a RuO_x particulate material of 100 m^2/g surface area should yield capacitances as high as 150 F/g. For a 20 mg/cm^2 RuO_x electrode structure this should give a calculated capacitance of 3 F/cm^2. The observed capacitance, however, is only $\backsim 1$ F/cm^2. Through TEM studies in the above cited reference it has been observed that for the RuO_x particles the typical particle diameter is approximately 50 000 Å with a porous substructure which is only partially accessible to the solid ionomer. Thus there is a significant portion of the 100 m^2/g surface area that is not available for capacitive charging. If the particle size of RuO_x is reduced to 40 Å size, then assuming spherical particles, and using eqn. (7),

$$\text{Surface area} = \frac{6}{\rho D} \qquad \begin{array}{l}\rho = 7 \text{ g/cc for } RuO_x \\ D = 40 \text{ Å (particle diameter)}\end{array} \tag{7}$$

a surface area of 214 m^2/g is calculated. Of more importance is that essentially all of the surface area of the 40 Å particle should be accessible for coating with solid ionomer. For this surface area, capacitances of the order of 320 F/g are obtainable. Assuming a 20 mg/cm^2 RuO_x electrode structure (40 Å particles coated with solid ionomer) the calculated capacitance is 6.4 F/cm^2.

Table 5 shows our initial results on our attempts to increase the specific capacitance. Two approaches have been experimented in obtaining the data presented in Table 5. The first two entries in this Table use RuO_x–IrO_x alloy and IrO_x pure material to enhance capacitance. The addition of IrO_x to RuO_x increases the surface area and, perhaps, results in increased specific capacitance. The capacitance of a solid-ionomer cell fabricated with IrO_x was 1.4 F/cm^2, leading to a specific capacitance of 45 F/g. The second approach is to disperse the RuO_x to 20–200 Å range particle size. To do this, we need to use a substrate on which the RuO_x can be deposited. Activated carbon was chosen as a support and RuO_x deposited onto it using various methods. The increase in specific capacitance is approximately one order of magnitude. One disadvantage in this approach is the loss of volume energy density. Approaches are being investigated to at least partially preserve the volume energy density while decreasing the RuO_x content.

Approaches to increasing low-temperature performance

The influence of temperature on the performance of a PEM all-solid ionomer capacitor is shown in Table 4. The capacitor contains only hydrated water which is part of the ionomer structure. The performance of these capacitors drops abruptly below the freezing point of water. Two factors appear to contribute to the performance decrease: the conductivity of the electrolyte and the rate of the proton transfer reaction.

$$RuO_x(OH)_y + H^+ + e^- = RuO_{x-1}(OH)_{y+1} \quad (8)$$

We attempted to improve the performance of these devices by lowering the freezing point of water through the addition of certain solutes.

Figure 6 shows the capacitance and ESR behavior as a function of temperature for MEAs treated in several ways. The capacitance of the baseline

TABLE 5

Approaches to increasing the specific capacitance of the all-solid ionomer capacitor

Type	Loading (mg/cm^2)	Internal resistance (Ω cm^2)	Capacitance (F/cm^2)	Capacitance (F/g metal)
RuO_x–IrO_x	5	0.25	0.40	40
IrO_x	16	1.25	1.40	45
5% RuO_x on carbon(I)	10	0.21	0.48	480
5% RuO_x on carbon(II)	20	0.60	0.75	375
5% RuO_x on carbon(III)	20	0.48	0.68	340
50% RuO_x/IrO_x on carbon	13	0.38	0.63	63

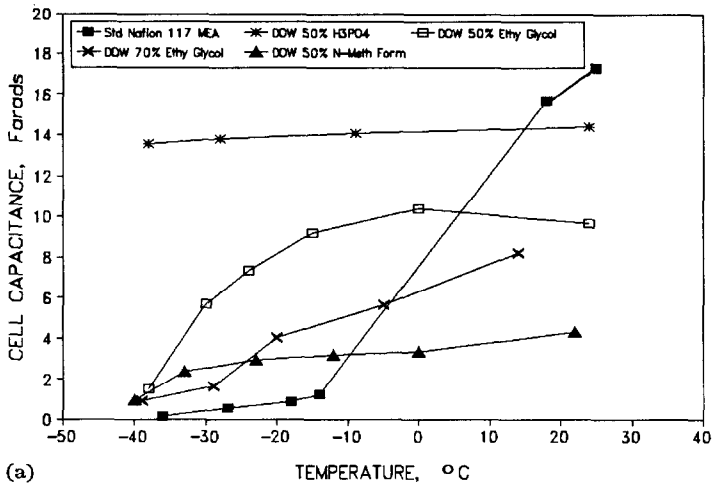

(a)

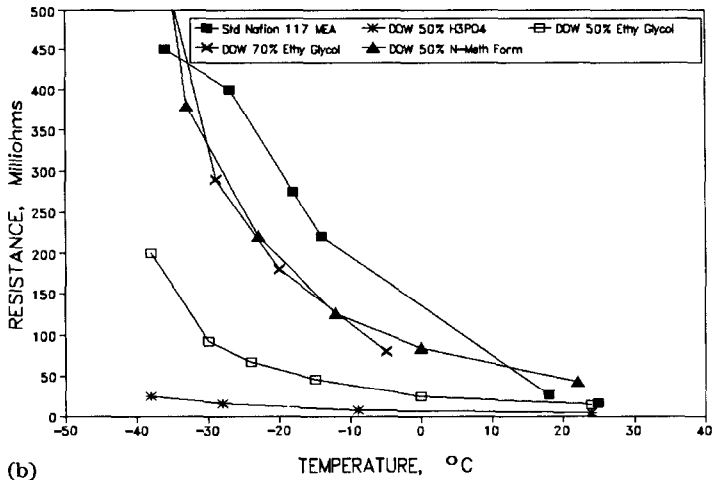

(b)

Fig. 6. Effect of variation in room-temperature treatment conditions of MEA capacitance and ESR behavior as a function of temperature of MEA operation, measured by discharge across 10 Ω (cell area = 25 cm^2). (a) Capacitance as a function of temperature. (b) Resistance as a function of temperature.

Nafion 117 MEA (contains only water) dropped drastically from 0.693 F/cm^2 at room temperature (25 °C) to 0.048 F/cm^2 at −14 °C, while internal resistance increased from 17 to 220 μΩ. The test results obtained after soaking the MEAs in phosphoric acid, glycol and *N*-methylformamide solution are summarized below.

DOW MEAs were tested after treating by soaking overnight in 43% H_3PO_4 (50% by volume solution of Fisher 85% phosphoric acid), 40%, 50% and 70% solutions of ethylene glycol (J. T. Baker no. 3-9300), and 50%

N-methylformamide, then tested at various temperatures down to approximately −40 °C to obtain performance curves. Treatments with all the solutions above were carried out at room temperature. Some testing was also conducted by soaking the MEAs in glycol solutions for 1 h at 25 °C. In one set of these experiments, a treatment solution containing 5% Nafion in glycol/water was used.

Phosphoric acid treatment of MEAs

The DOW MEA treated in 43% H_3PO_4 was clearly superior at retaining capacitance and internal resistance characteristics. From 25 °C down to −38 °C, capacitance dropped from 0.577 to 0.543 F/cm^2 (94% retention) while internal resistance rose from 4.2 to 25 $\mu\Omega$.

Ethylene glycol treatment of MEAs

The MEAs treated with 40% and 50% ethylene glycol in water for 1 h at 25 °C appear to show good low-temperature performance as shown in Fig. 7. Also included in these tests was a MEA treatment with a 5% Nafion ionomer in 50/50 glycol water. The 40% ethylene glycol in water showed the best overall capacitance from 25 °C down to a temperature of approximately −25 °C. From 25 °C down to −20 °C, capacitance dropped from 0.701 to 0.532 F/cm^2 (76% retention). However, at a temperature of −30 °C, capacitance dropped to 0.164 F/cm^2. The effect of using (i) 50% ethylene glycol in water and (ii) 5% Nafion ionomer in the 50/50 glycol/water is also shown in Fig. 7. The capacitance data for the MEA soaked in 50% glycol in water have been normalized for making a direct comparison of the data. It appears some improvement in −30 °C low-temperature performance for the glycol systems is obtained when using 50% rather than 40% glycol in water. Addition of dissolved Nafion ionomer (5%) to the 50% glycol solution appears to improve the MEA performance compared to the 50% glycol alone. Further work is required to define the optimum water/glycol ratio and treatment conditions. A potential advantage of the water/glycol system versus the H_3PO_4 system for improving low-temperature capacitor performance is that the glycol is not a liquid electrolyte, thus minimizing the possibility of shunt currents, corrosion and leakage.

N-Methylformamide treatment of MEAs

The performance of an MEA soaked in a 50% *N*-methylformamide solution is shown in Fig. 6. Generally, the overall performance of the cell as to capacitance and resistance was poor, compared to the H_3PO_4 and the 40%, 50% glycol solutions.

A summary of the low-temperature results is shown in Table 6. In the above experiments, we have used a new MEA for each low-temperature experiment in order to avoid contamination from one experiment to another. However, the capacitance of the several MEAs used in this test program varied somewhat. The best low-temperature results were obtained for phosphoric acid; the capacitance value at −30 °C for the MEA soaked in phosphoric

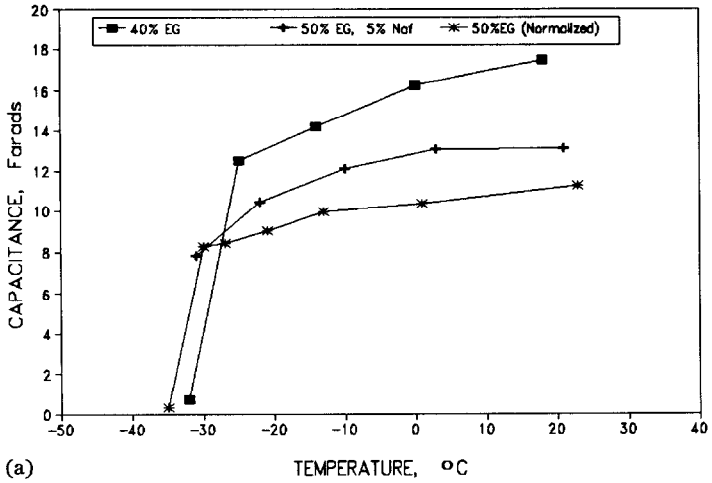

(a)

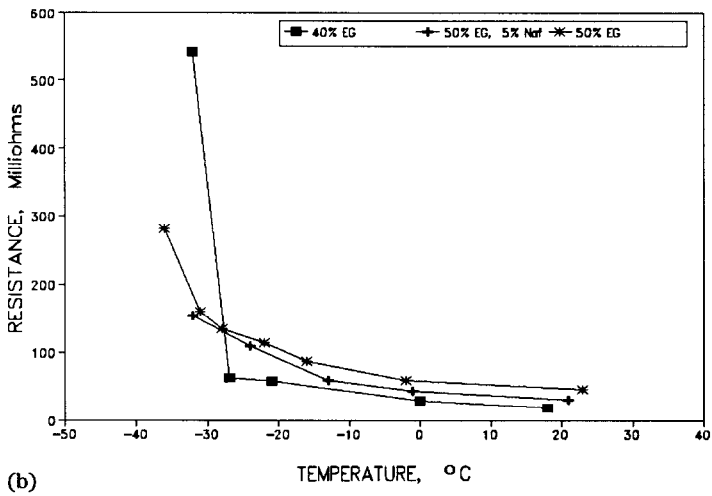

(b)

Fig. 7. Effect of short-term, room-temperature treatment in glycol–water mixtures (with and without Nafion) on MEA capacitance and resistance as a function of MEA operation, measured by discharge across 10 Ω (cell area = 25 cm^2). (a) Capacitance as a function of temperature. (b) Resistance as a function of temperature.

acid is approximately 95% of the 25 °C value. Both 40 and 50% ethylene glycol treated samples retain 60–80% at −20 °C of the 25 °C capacitance; however at −30 °C, 50% glycol shows better performance.

Aerospace applications

Although the projected energy densities for electrochemical capacitors are about two orders of magnitude lower than that of batteries, the high-power-density characteristics of these devices renders them as potentially

TABLE 6

Comparison of room temperature vs. low temperature performance for capacitors treated with various solvents

Treatment				Before treatment		After treatment					
Solution	Concentration (%)	Temperature (°C)	Time (h)	25 °C		25 °C		−20 °C		−30 °C	
				ESR[a]	C[b]	ESR	C	ESR	C	ESR	C
H_3PO_4	43	25	20	5	0.505	4.2	0.577	11	0.556	17	0.549
Ethylene glycol	50	25	20	5	0.529	14	0.386	55	0.327	92	0.227
Ethylene glycol	70	25	20	5	0.529	–	–	180	0.161	337	0.063
N-Methylformamide	50	25	20	5	0.527	42	0.172	194	0.120	332	0.101
Ethylene glycol	40	25	1	6	0.614	19	0.701	57	0.532	410	0.164
Ethylene glycol, 5% NAF	50	25	1	6	0.586	31	0.525	92	0.428	144	0.324
Ethylene glycol	50	25	1	5.5	0.586[c]	46	0.450[c]	105	0.367[c]	152	0.331[c]

[a]In $\mu\Omega$. [b]In F/cm^2. [c]Normalized.

viable candidates for meeting pulse or peak electrical power requirements for some anticipated aerospace mission scenarios, especially those with discharge times on the millisecond to second time scale. On a volumetric or gravimetric basis, the advantages of utilizing electrochemical capacitors rather than batteries for meeting the peak power demands associated with a specific mission scenario will largely depend upon the total and pulse durations of the power peaks.

Projected energy and power densities for electrochemical capacitors and batteries [25] can be used to make approximate volumetric comparisons between these two power sources for peaking applications. For example, for a defined peak power level and total duration, the total energy required for storage in an electrochemical capacitor can be calculated. If one assumes that the total charge will be stored in the cell structure of the capacitor, then the volume of the capacitor which satisfies both its energy and power density characteristics can be estimated. A similar calculation can be made to estimate the volume of the reserve portion of a battery power source, i.e. the additional size to meet the peaking demands which exceed the steady-state power needs. Based on the data cited above, the estimated volumes of an electrochemical capacitor and a battery for supplying the peak power needs would be equal for a total peak power duration of 2.0 min. For a total duration of 30 s, the volume of a battery peaking power source would be four times larger than that of an electrochemical capacitor. If a mission scenario is such that there is sufficient time for recharging between transients, then the required capacitor volume could be reduced even further.

Besides the potential for volume and/or mass reductions, other inherent characteristics of electrochemical capacitors could be critical drivers for selection of this technology for specific missions. High reliability and safety have significant impact on technology selection, and solid-ionomer electrochemical capacitors contain no toxic or corrosive electrolyte nor are any appreciable reaction products formed. They have a very high cycle life, and thus, can be utilized as a rechargeable secondary power source, if this is a feasible option for a mission scenario. Assessments of power source technologies will also need to consider effects of the thermal environment which will be encountered upon the power source, as well as any operational constraints which may be imposed by incorporation of the power source in high-speed circuitry.

Specific applications for electrochemical capacitor technology may be envisioned within the advanced launch systems (ALS) development and Orbiter upgrade programs which are presently being pursued within NASA. With such goals as increasing safety, reducing turnaround time, lowering recurring costs, reducing vehicle weight, and increasing operational efficiency in mind, a major objective of these programs is to replace existing auxiliary power unit (APU)/hydraulic actuator systems with electromechanical actuator (EMA) systems.

An advanced EMA system, which is depicted in Fig. 8, will require a highly reliable power source to meet its unique electrical power requirements,

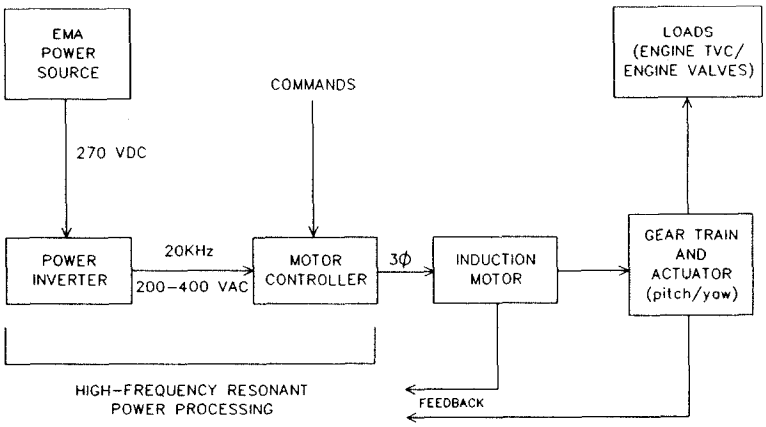

Fig. 8. Electrochemical actuator (EMA) system elements.

which include high peak power pulses for short durations (< 100 ms). The advanced EMA system, which would be composed of independent power channels to meet failure-tolerant design requirements, would be developed to have high-power and high switching-speed capabilities. Multi-phase induction motors would be controlled via a high-frequency a.c. link using resonant power processing technology. For shuttle evolution programs, the proposed EMA system would power and control all the flight control surfaces, landing gear, and the Orbiter's thrust vector control (TVC) systems. These systems are powered just before launch, during ascent, and throughout re-entry and roll-out.

As part of a Shuttle EMA system study performed for the Johnson Space Center, several candidate electrical power system configurations were conceived to meet EMA power requirements and were compared to determine which would be the most suitable option [26]. The electrical power requirements per power channel which were used to synthesize the power systems included:

3.5 kW average power
5.5 kW h energy
120 kW peak power (400 ms total; 40–80 ms pulses)
270 VDC

The candidates for the conceptual study included several high-power-density battery systems, modified Orbiter fuel cells in both dedicated and integrated design approaches, and advanced (high power density) alkaline fuel cells.

In the above study, the modified Orbiter fuel cell design approaches were favored with respect to imposing the least impact upon the implementation schedule and initial cost of implementation. Both of the conceptual design approaches incorporated the solid-ionomer electrochemical capacitor for

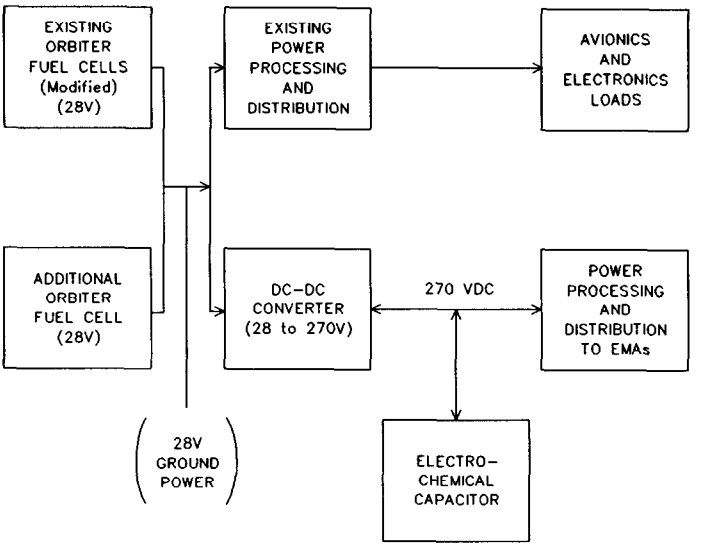

Fig. 9. Schematic of an integrated Orbiter fuel cell design approach for meeting EMA power requirements.

providing the 120 kW peak power pulses specified for the ascent and descent phases of EMA operation. The scaled-up 270 V capacitor required per power channel, which was sized based upon existing data, would contain 300 cells, weigh approximately 60 lbs, and occupy a volume of approximately 0.5 ft^3. A schematic of an integrated design approach is shown in Fig. 9.

As mentioned earlier, the replacement of hydraulic actuators with EMA systems is also a critical element in NASA's ALS programme, which addresses TVC technology for solid rocket boosters, Atlas/Centaur launch vehicles, etc. Electrical power system trade studies have also been performed within this program, and candidate power sources have included high-rate primary and secondary batteries, fuel cells, turboalternator systems and flywheel energy storage systems [27]. The recommended system for development based on these studies, which did not include electrochemical capacitor technology, was the bipolar lead/acid battery. The electrochemical capacitor could prove to be a viable competitor for meeting peak power demands, and an approach incorporating electrochemical capacitor technology needs to be evaluated with respect to satisfying overall mission requirements.

Conclusions

Life testing of a multicell capacitor on an intermittent basis has shown that, over a 10 000-h period, the capacitance and resistance of the cell has remained invariant. There has been no maintenance required on the device since it was fabricated. Other multicell units of shorter-life duration have exhibited similar reliable performance characteristics.

The results obtained with multicell solid-ionomer electrochemical capacitors indicate gravimetric and volumetric power densities in the range of 2×10^3 W/g and 4×10^4 W/l, respectively, can be obtained for 5 ms pulses. Initial testing indicates that the specific capacitance of these devices can be further increased by (i) use of additives, or alloying of the RuO_x particles to result in a higher-surface-area particulate electrode structure and (ii) dispersion of the RuO_x to the 20–200 Å range particle size by depositing the RuO_x on high-surface-area carbon. This should result in further increase in power and energy densities. Further work in this area is recommended.

Testing indicates there is loss in efficiency (joules out/joules in) when discharging the capacitor devices across a low-resistance load. The efficiency decreases from 83% for a 10 Ω load to 35% for a 0.134 Ω load. The formation of smaller RuO_x particles (20–200 Å) and improved ionomer coating should help access more of the RuO_x surface structure and improve efficiency. Some initial testing of the self-discharge characteristics of the solid-ionomer capacitor indicate that approximately 15% of the energy if lost for a holding time of 5 min. This loss can likely be decreased by using improved quality procedures when fabricating the individual cells to minimize electrical shunt paths.

The performance of the solid-ionomer capacitor, containing only hydrated water, drops abruptly below the freezing point of water. Two factors appear to contribute to the performance decrease: the conductivity of the electrolyte and the proton transfer reaction. The performance of the capacitors was improved by lowering the freezing point of water through the addition of certain solutes. Addition of phosphoric acid to the MEAs extends the low-temperature limit of our capacitors to −30 °C, without any significant loss in performance. Treatment of the MEAs with certain concentrations of glycol in water also improves the low-temperature performance significantly compared to the baseline MEA. The low-temperature performance of capacitors equilibrated with glycol appears to depend on the quantity of glycol in the membrane and treatment conditions. A range of 40–50% glycol in water and 1 h treatment at 25 °C gave the best results in this study. The addition of dissolved Nafion ionomer (5%) to the 50% glycol solution appears to improve MEA performance compared to 50% glycol alone. A potential advantage of the water/glycol system versus the H_3PO_4 system for improving low-temperature capacitor performance, is that the glycol is not a liquid electrolyte, thus minimizing the possibility of shunt currents, corrosion and leakage. A systematic study of the proton mobility and ionic conductance at low temperatures in proton-exchange membranes equilibrated with different types and quantities of non-electrolyte solutes may lead to optimum low-temperature behavior of our capacitors and is recommended for future studies.

Acknowledgements

This work was supported in part by the following: DARPA/Office of Naval Research Contract N00014-88-C-0391, Sandia National Laboratories,

and National Science Foundation Grant ISI-9060142. The authors express their thanks to Dr J. Giner for several interesting discussions based on which the material in the 'Introduction' was developed.

References

1 D. L. Boos, *U.S. Patent No. 3 536 963* (Oct. 27, 1970).
2 J. Phillips and H. Takei, *U.S. Patent No. 4 438 481* (Mar. 20, 1984)
3 E. A. Cuellar and M. J. Desmond, *U.S. Patent No. 4 630 176* (Dec. 16, 1986).
4 J. C. Currie, *US Army Workshop on Capacitors and Batteries for Pulse Power Application, Asbury Park, NJ, 1987*, p. 211.
5 M. F. Rose, S. Best and B. Tatarchuk, *US Army Workshop on Capacitors and Batteries for Pulse Power Applications, Asbury Park, NJ, 1987*, p. 249.
6 F. Rose, D. Kohler and B. Tatarchuk, *J. Electrochem. Soc., 137* (1990) 6.
7 K. Hiratsuka, T. Morimoto, Y. Sanada and K. Kurihara, *Ext. Abstr., Electrochemical Society Meet., Seattle, WA, 1990*, p. 129.
8 J. M. Kleijn and J. Lyklema, *J. Colloid Interf. Sci., 120* (1987) 511.
9 G. L. Holleck, B. H. Jackman and R. D. Rauh, *173rd Electrochemical Society Meet., Atlanta, GA, May 1988*, Abstr. no. 18.
10 Ho-Lun Lee, G. Mason and K. Kern, *Final Rep., Contract No. N00014-87-C-0705*, Office of Naval Research, Arlington, VA, 1988.
11 S. Trasatti and G. Lodi, in S. Trasatti (ed.), *Electrodes of Conductive Metallic Oxides*, Part A, Elsevier, Amsterdam, 1980, Ch. 7.
12 E. N. Balko, C. R. Davidson and A. B. LaConti, *J. Inorg. Nucl. Chem., 42* (1980) 1778.
13 T. G. Coker, R. M. Dempsey and A. B. LaConti, *U.S. Patent No. 4 191 618* (1980).
14 D. R. Craig, *Can. Patent No. 1 196 683* (1985)
15 H. B. Sierra Alc-zar, K. A. Kern, G. E. Mason and R. Tong, *Proc. 33rd Int. Power Sources Symp., June 13–16, 1988*, The Electrochemical Society, Pennington, NJ, 1988, p. 607.
16 J. McHardy, *US Army Workshop on Capacitors and Batteries for Pulse Power Applications, Asbury Park, NJ, 1987*, p. 277.
17 J. McHardy, F. A. Ludwig, L. R. Higley, A. Kindler and C. W. Townsend, *U.S. Patent No. 4 766 522* (1988).
18 R. D. Rauh, *US Army Workshop on Capacitors and Batteries for Pulse Power Applications, Asbury Park, NJ, 1987a*, p. 408.
19 R. D. Rauh, *Final Rep., Contract No. N00014-86-C-0803*, Office of Naval Research, Arlington, VA, 1987b.
20 D. A. Corrigan, *J. Power Sources, 21* (1987) 33.
21 S. Glarum and J. Marshall, *J. Electrochem. Soc., 134* (1987) 2160.
22 G. Gottesfeld, A. Redondo and S. W. Feldberg, *Ext. Abstr., Electrochemical Society Meet., San Diego, CA, 1986*, Abstr. no. 507.
23 S. D. Bhakta, D. D. Macdonald and S. C. Narang, *Ext. Abstr., Electrochemical Society Meet., Seattle, WA*, Vol. 90-2, The Electrochemical Society, Pennington, NJ, 1990.
24 S. Sarangapani, P. Lessner, J. Forchione, A. Griffith and A. B. LaConti, *J. Power Sources, 29* (1990a) 355.
25 S. Sarangapani, P. Lessner, J. Forchione, A. Griffith and A. B. LaConti, *Proc. 25th Intersociety Energy Conversion Engineering Conf.*, Vol. 3, 1990b, p. 137.
26 H. McBryar, personal communication, 1991.
27 L. Burrows, personal communication, 1991.